MULTIFRAGMENTATION IN HEAVY ION NUCLEAR REACTIONS

A thesis

Submitted in the partial fulfillment of requirement for the award of the degree of

Master of Science

In

Physics

Submitted by:

Ravinder Goyal

Regn. No.-30704014

Under the esteemed guidance of

Dr. Suneel Kumar

School of Physics and Material sciences

THAPAR UNIVERSITY

PATIALA-147004

JUNE-2009

CERTIFICATE

I hereby certify that the work, which is being presented in the thesis, entitled "Multifragmentation in heavy ion reactions" in partial fulfillment of the requirements for the award of degree of Master of Science in Physics at Thapar University, Patiala, is an authentic record of my own work carried out under the supervision of Dr. Suneel Kumar. I have not submitted the matter presented in the thesis for the award of any other degree of this or any other university.

Ravinder Goyal

(Ravinder Goyal)

This is to certify that the above statement made by the candidate is correct and true to best of my knowledge.

S Kumar

Supervisor

Dr. Suneel Kumar

School of Physics and Material Sciences

Thapar University

Patiala

Countersigned by:

O. Mar

Dr. O.P. Pandey

Professor and Head

SPMS

Thapar University

Patiala.

RK Sharma 22/6/09

Dr. R.K. Sharma

Dean of academic affairs

Thapar University

Patiala.

ACKNOWLEDGEMENT

This thesis is the beginning of my ride to intellectual sorority and blossom my innate thoughts. I have not traveled in a vacuum in this journey. There are some people who made this journey easier with words of encouragement and more intellectually satisfying by offering different places to look to expand my theories and ideas.

First a very special thanks to my supervisor ***Dr. Suneel Kumar*** who gave me the confidence and support to begin my Master's program and helped me to set my benchmark even higher and to look for solutions to problems rather than focus on the problem. I learned to believe in my future, my work and myself.

I also thank ***Dr. O.P. Pandey***, Professor and Head, School of Physics and Material Science for his support and providing facilities.

It gives me a great pleasure to thank ***Mr. Sanjeev Kumar*** for his constant encouragement and unending support and from whom I have learnt the art of working on tasks with constructive efforts.

My sincere thanks to all the office staff who had made my life easier by providing me assistance in all times of need.

I would also like to gratefully acknowledge the support of my classmates. They helped me immensely by giving me encouragement and friendship. They mirrored back my ideas so I heard them aloud, an important process for me to shape this thesis and future work.

Finally, I wish to express my profound regards to my parents without whose constant encouragement and support, I would not have made it this echelon.

PLACE: TIET PATIALA RAVINDER GOYAL
DATE

ABSTRACT

The present work deals with the theoretical study of multifragmentation and it's associated phenomena in heavy-ion collisions. Firstly, we give some details about the experiments, their theoretical concepts and experimental set ups held in past years in which multifragmentation data obtained at the SIS/GSI accelerator is reviewed using heavy ion beams with (0.1-1)A GeV together with the ALADIN and FOPI experimental setups. After that, we discuss various models used to study multifragmentation in recent years. This work is done within the framework of *Quantum Molecular Dynamics (QMD)* model. This model allows to study the influence of several types of nucleonic interactions on a large variety of observables and phenomena occurring in heavy ion collisions at relativistic energies. Finally, we give qualitative analysis of various results obtained theoretically in multifragmentation and also compare some of our results with those obtained experimentally from ALADIN experiment.

TABLE OF CONTENTS

Chapter 1

Introduction

Multifragmentation is the dominant decay mode of heavy nuclear systems with excitation energies in the vicinity of their binding energy. It explores the partition space associated with the number of nucleonic constituents and it is characterized by a multiple production of nuclear fragments with intermediate mass. Reactions at relativistic bombarding energies, exceeding several hundreds of MeV per nucleon, have been very efficient in creating such highly excited systems. Peripheral collisions of heavy symmetric systems or more central collisions of mass asymmetric systems produce spectator nuclei with properties indicating a degree of equilibration. The observed decay patterns are well described by statistical multifragmentation models. The present experimental and theoretical studies are particularly motivated by the fact that multifragmentation is being considered a possible manifestation of the liquid gas phase transition in finite nuclear systems. [1] From the simultaneous measurements of the temperature and of the energy content of excited spectator systems a caloric curve of nuclei has been obtained. The characteristic S-shaped behavior resembles that of ordinary liquid.

Signatures of critical phenomena in finite nuclear systems are searched for in multifragmentation data. These studies, supported by the success of percolation in reproducing the experimental mass or charge correlations, concentrate on the fluctuations observed in these observables. Attempts have been made to deduce critical point exponents associated with multifragmentation.

The hope to establish a link to the liquid-gas phase transition in nuclear matter has been a major motivation for the search for and the study of multifragment decays of heavy nuclei in recent years. Multifragmentation was predicted to be the dominant decay mode at excitation energies near the binding energy of nuclei of about 8 MeV per nucleon and at densities below the saturation density of nuclear

matter [2,3]. These conditions of high excitation and low density coincide with the liquid gas coexistence region as predicted for nuclear matter from the Van-der-waals type range dependence of the nuclear forces. It was also suggested early on that this region may be explored during the later stages of energetic nuclear reactions.

The experimental study of the nuclear liquid-gas phase transition in finite nuclei faces several serious difficulties related to the fact that excited nuclei are composed of a small number of constituents, that they are charged, and that there is no external pressure to counteract the internal pressure of the system at a given equilibrium condition [4]. Finite pressure may be maintained only dynamically and for very short periods of time during the disintegration process. There is also no heat bath available which would allow predetermining the temperature of the system in order to measure its response to it.

In spite of these difficulties, stimulating new results have been presented very recently. They suggest that signals of nuclear liquid gas phase transition may be revealed by studying reactions of finite nuclei. From the simultaneous measurement of the temperature and the excitation energy for excited projectile spectators in ^{197}Au+^{197}Au collisions at 600 MeV per nucleon a caloric curve of nuclei has been obtained. It exhibits a typical S-shaped behavior, reminiscent of first-order phase transitions in macroscopic systems. For the ^{197}Au on C reaction at 1.0 GeV per nucleon, the EOS collaboration has reported values of critical-point exponents which were derived from the correlation and fluctuations of the fragment sizes [5]. In both cases, the data providing the basis for the analysis were obtained from the fragmentation of heavy projectiles at relativistic energies in the range of upto about 1 GeV per nucleon. The decay properties of spectator nuclei produced in these reactions indicate that a high degree of equilibrium has been reached. This is a prerequisite for the study of the thermodynamic behavior of highly excited nuclear matter and makes these reactions rather attractive for this purpose.

1.1 Experimental setups

Statistical approaches have been invoked from the beginning in order to try to understand the experimental data in multifragmentation. Evidence for non-equilibrium effects lead to the parallel development of sophisticated transport models as well. The many facets of multifragmentation are studied in laboratories all over the world. We describe the ALADIN and FOPI experimental setups as below.

The ALADIN [6] spectrometer (shown in fig. 1.1) was designed primarily to look at fast projectile-like spectator fragments focused into a forward cone of about $\pm 5^{o}$. In some experiments complementary detectors are installed, such as a large area neutron detector LAND that identifies neutrons emitted close to 0^{o}, and a series of multidetector hodoscopes consisting of Si-Cs(Tl) telescopes, CaF_2 plastic phoswich detectors and Si-strip detectors arranged so as to cover angles between $6^{o} - 58^{o}$. One of the purposes of the TP-MUSIC detector is to allow precise tracking of charged particles passing through its active volume. The version MUSIC-II [7] is shown in Fig. 1.3.

Two large detection systems have been set up at the heavy ion synchrotron SIS at GSI Darmstadt, ALADIN (Fig. 1.1) and FOPI (Fig. 1.2).

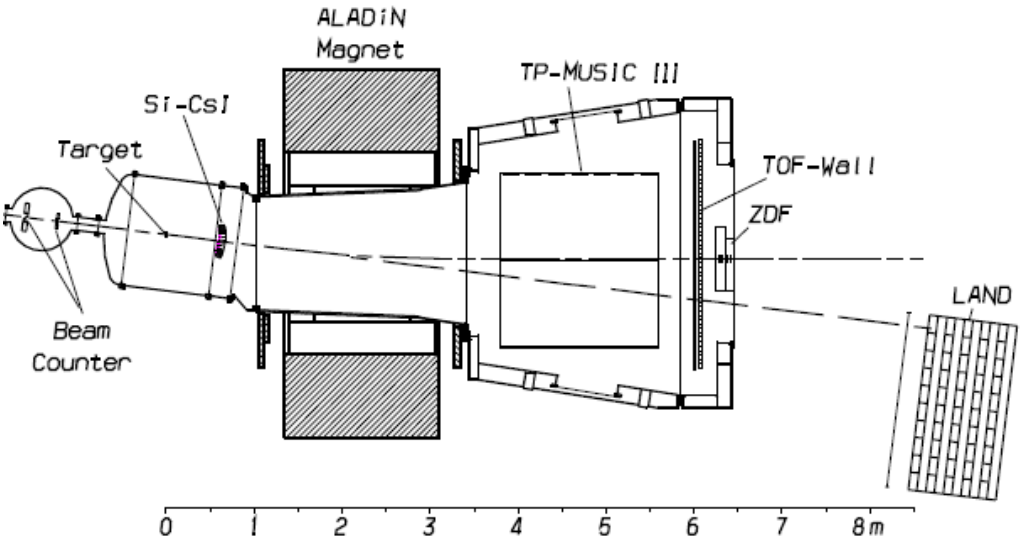

Figure 1.1: Schematic view of the ALADIN spectrometer in the bending plane [4].

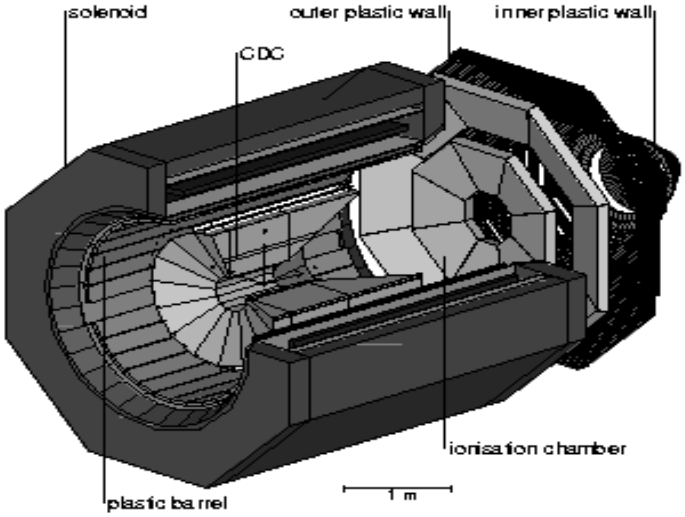

Figure 1.2: Schematic view of the FOPI detector.

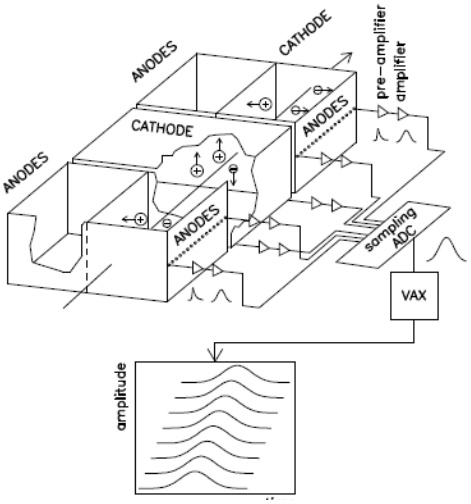

Figure 1.3: Illustration of the operation of the MUSIC II detector [7]

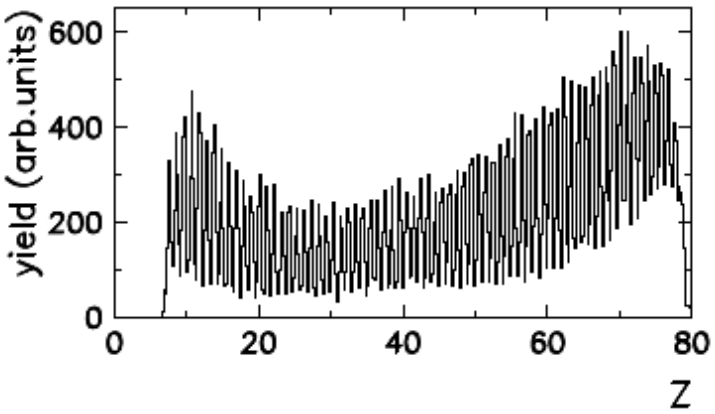

Figure 1.4: Observed charge spectrum [7]

It consists of three active volumes with the electric drift fields in adjacent sections perpendicular to each other, two for the measurement of the horizontal and one for that of the vertical position and angle of the particle track. To allow multiple sampling of the particle signals, each anode is subdivided into 16 stripes with a width of 3 cm each. The anode signals are recorded using flash analog-to-digital converters (ADCs) with a sampling rate of 16 MHz. Better than unit resolution for nuclear charges from Z=8 all the way to Au (Z=79) is

obtained (Fig. 1.4). Charges between Z=2 and 15 can be resolved with use of the scintillator strips in the TOF.

The FOPI apparatus was built to study central heavy ion reactions in the energy range 0.1-2A GeV. Particle identification, again, is done by a combined energy-loss, time-of-flight and magnetic rigidity analysis. The magnet is a superconducting solenoid operated at 0.6 T (see Fig. 1.2). Time of flight and energy-loss are determined by about 1000 scintillator detectors arranged octogonally in the downstream part of the detector (PLASTIC WALL) and as a barrel inside the magnet. At lower incident energies (E/A $\leq$400 MeV) a set of gas ionization chambers is inserted in front of the PLASTIC WALL to allow identification of slower heavy clusters (up to Z about 15). Inside the magnet, the particles are tracked in drift chambers, the Central Drift Chamber, CDC, and the HELITRON (usually installed in front of the CDC, but not shown here). Fig. 1.5 allows to visualize individual particle tracks in a specific event determined with use of local or global (Hough transform) track finding methods.

By matching these tracks to the outer barrel scintillators one obtains the energy loss (from the ionization in the CDC gas), the track curvature and the time-of-flight (from the Barrel).

A systematic analysis of the Multifragmentation (MF) in fully reconstructed events from 1A GeV Au, La and Kr collisions with C has been performed. Detailed comparisons of the various fragment properties are presented as a function of excitation energy, E_{th}. The charged particle multiplicity from MF stage shows saturation beyond $E_{th\sim}$8 MeV/nucleon for Kr. The universal behavior of intermediate mass fragment yields and of the size of the largest fragment is observed only for Au and La when scaled with size of the system. The Kr data are found to lack this property. Moments of the fragment size distribution show that the Kr MF is different than the MF of Au and La. A power law behavior is observed for Au and La with exponent $\tau > 2$, while for Kr $\tau < 2$. The results are compared with the statistical multifragmentation model (SMM). A single value of all the parameters of the model fits the data for all the three systems.

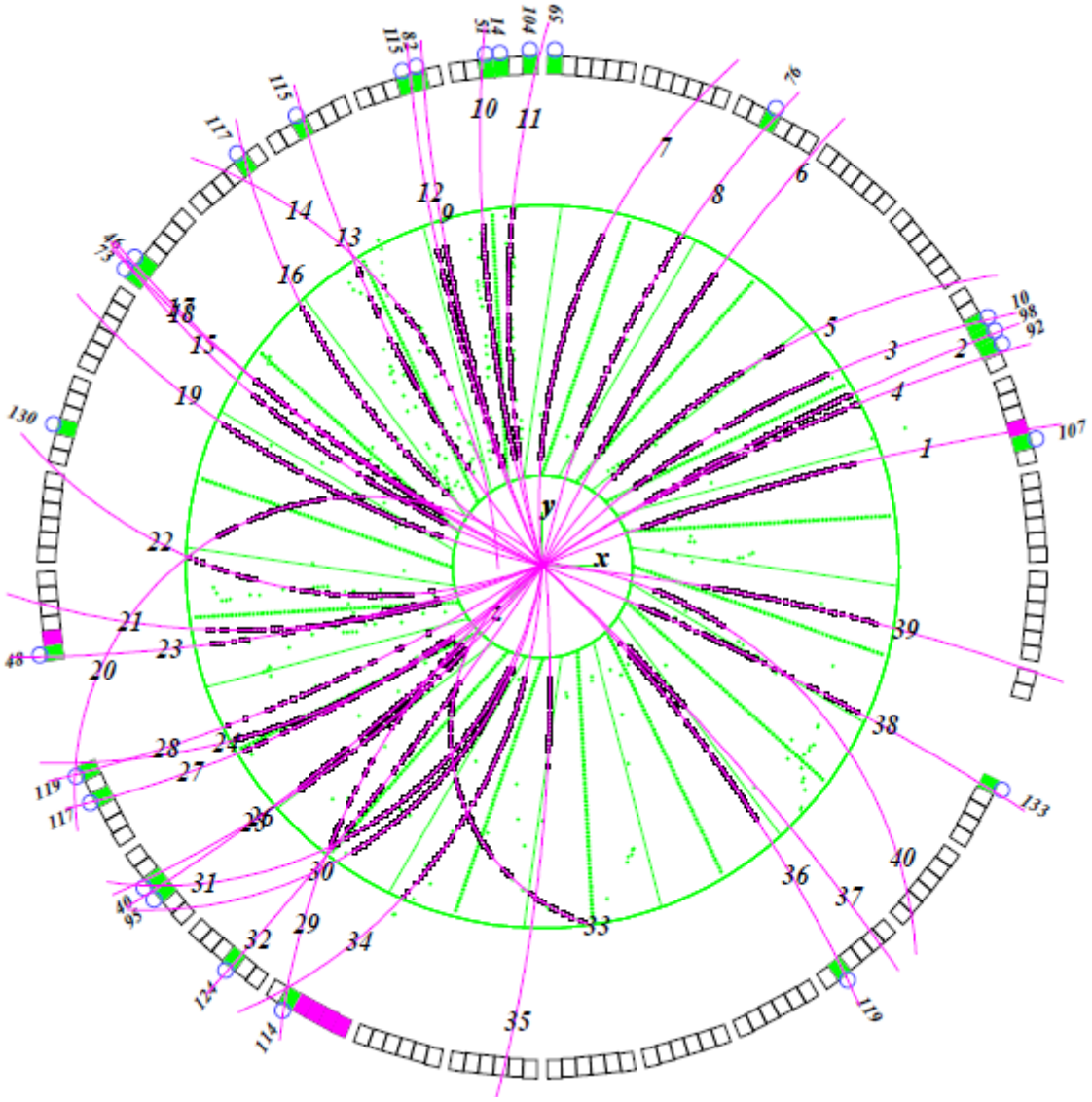

Figure 1.5: Event display in the Central Drift Chamber. A cross section in the plane perpendicular to the beam axis is shown

The breakup of Au and La is consistent with a continuous phase transition. The data indicate that both E_{th} and the isotope ratio temperature $T_{HE\text{-}DT}$ decrease with increase in system size at the critical point. The breakup temperature obtained from SMM also shows the same trend as seen in data. This trend is attributed primarily to the increasing Coulomb energy with finite size effects playing a smaller role. The percolation and Ising model studies for finite size neutral matter show behavior which is opposite to the one seen in the present day work.

During the past decade a large effort has been made to understand the multifragmentation (MF) process in heavy ion reactions. The Purdue group was the first to suggest that nuclear MF might be a critical phenomenon – a second order phase transition occuring near a critical point [8,9]. The discovery that the yields of fragments with mass A_f produced in p + Kr and p + Xe reactions, with proton beam energy from 80 to 350 GeV, obeyed a power law Y (A_f)~$A_f^{-\tau}$, with $\boldsymbol{\tau}$~2.5 [9] generated theoretical interest in MF in terms of a continuous phase transition. A similar power law was also predicted by Fisher [10] for a mass distribution of droplets at a liquid–gas phase transition critical point. Another important result was the observation that MF is high energy phenomenon involving excitation energies of the order of the binding energy [11]. These observations suggested that MF was both a thermal process and might be related to the critical phenomena. In recent years further progress was made by experimentalists in which practically all the fragments emitted in a given event were detected, thereby permitting complete reconstruction of MF events. The EOS collaboration studied the MF of 1A GeV gold on carbon and analyzed the data using methods developed in the study of critical phenomena [12–17]. Several critical exponents were determined and their values suggested that the MF of Au can be understood as due to a continuous phase transition. In contrast to a liquid–gas phase transition, the MF transition appears to involve the breakup of a nucleus to form several IMF's. The production of nucleon and light particles – the nuclear analog of a gas occurs largely in the fragment de-excitation step [18]. Along with the earlier inclusive studies, these experiments suggested that prior to MF the remnant formed in the prompt stage achieves thermal equilibrium. A two step process was proposed for the collision. In the first prompt stage nucleons are knocked out of the participants. The emission of these prompt particles leaves a equilibrated remnant nucleus which undergoes de-excitation in a second step. The result from the EOS indicate that it would be appropriate to compare the EOS results with statistical models.

There are several statistical models which have been used to study MF, [19–21] but the most widely used are the statistical multifragmentation model (SMM) [19] and Monte Carlo micro canonical model (MMMC) [20]. The theoretical interest in MF is not confined to only statistical models but several other approaches to study MF have been

carried out e.g. percolation, lattice gauge and Ising models [22–24].This model is in good agreement with a variety of results for the MF of 1A GeV Au.

Besides a lot of work being done in this area there are so many queries related to Multifragmentation, like why do nuclei break into several fragments ? How and when they are formed ? What is the mechanism behind Multifragmentation ? Why does a nucleus shatter into several fragments if hit by a projectile ? Is this a statistical process making new micro-canonical phase space models the proper tool for its description or is it dynamical process ? etc. The answers to these queries are given timely making different improvements to the previous findings.

Two roads are presently being followed in order to establish the existence of a liquid- gas phase transition in finite nuclear systems from nuclear reactions at high energy. The clean experiment of observing the thermodynamic properties of a finite number of nucleons in a container is presently only possible with the computer. Performed with advanced nuclear transport models, it has revealed the first-order character of the transition and allowed the extraction of the pertinent thermodynamic parameters. The validity of the applied theory is being confirmed by comparing its predictions for heavy-ion reactions with exclusive experiments. The second approach is experimentally more direct. Signals of the transition are searched for by analysing reaction data within the framework of thermodynamics of small systems. A variety of potential signals has been investigated and found to be qualitatively consistent with the expectations for the phase transition. Many of them are well reproduced with percolation models which places the nuclear fragmentation into the more general context of partitioning phenomena in finite systems. A wealth of new data on this subject has been obtained in recent experiments, some of them with a new generation of multi-detector devices aiming at higher resolutions, isotopic identification of the fragments, and the coincident detection of neutrons. Isotopic effects in multifragmentation were addressed quite intensively, with particular attention being given to their relation to the symmetry energy and its dependence on density.

With the passage of time, one was able to accelerate the heavy ions with bombarding energies comparable to its rest mass. This opened up new dimensions which are termed as intermediate and relativistic energy heavy ion physics. Due to

formation of compressed and hot piece of nuclear matter at intermediate and relativistic energies, it gives possibilities to study the properties of nuclear matter at extreme conditions. The study of the behavior of hadrons in hot and dense matter is one of the central topics of present day research. Naturally like all other materials, the properties of nuclear matter are also influenced by the pressure, density and temperature. The hadronic matter may have a rich structure in this unexplored domain of high excitation energies and compressions. As indicated in figure 1.6, there are conjunctions about a nuclear liquid-vapour phase transition at low temperature and sub-nucleonic densities. At very high densities and temperatures, one may have the quark-gluon plasma [25,26,27]. Whereas at moderate temperatures, the hadron gas can occur.

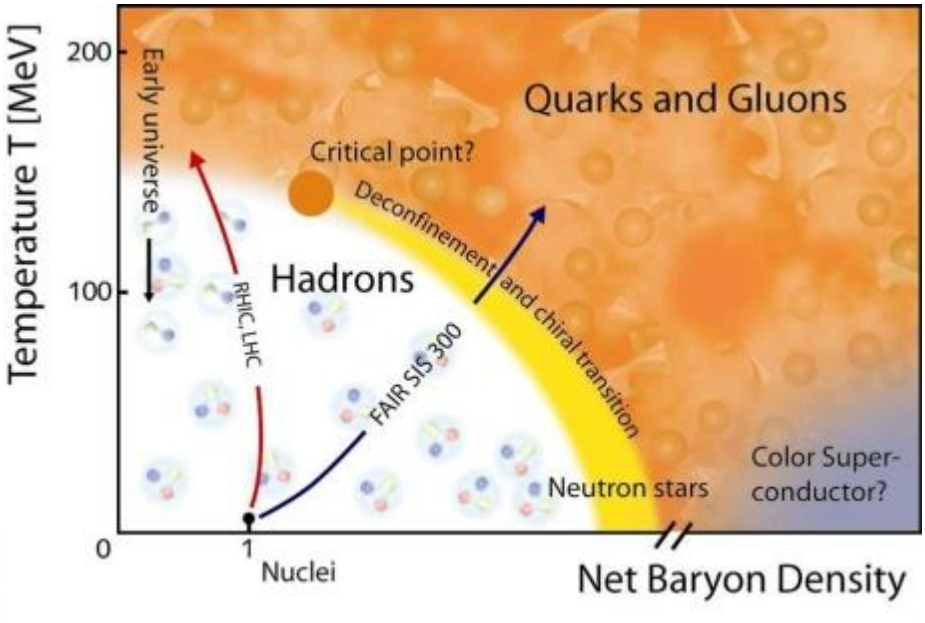

Fig1.6: Phase diagram of nuclear matter shows the fundamentally different states that have been conjectured. Experimentally, only the point (1,0) is known [26].

In the following we summarise the experiments which are performed during previous years and then a brief discussion of various theoretical methods will also be made.

The first experiments at Berkley served mainly to get the experimentalists and theoreticians aware of the problems and pitfalls of the way from medium energy heavy ion collisions to the equation of state. Later on, several accelerators were built at Michigan

state university (USA), GANIL (Germany). The SIS (heavy ion synchrotron) accelerator at GSI is specifically designed to study the heavy ion collisions at intermediate energies. The MSU group at Michigan state university is very active in studying the fragment's spectra at lower side of bombarding energies. The similar efforts are also made by the INDRA group at GANIL. The ALADIN group at GSI has gone ahead and provided a complete spectra of the fragments. These measurements include the incident energies up to 1A GeV.

The INDRA collaboration at GANIL is studying mainly the collisions where large multiplicities of the nucleons are observed in exit channel. They have undertaken a wide program where influence of different parameters on multi-fragmentation is studied. Note that these parameters include the role of size of system in entrance channel. (incident energies and mass asymmetry), the Coulomb instabilities etc. in particular, the size effects are studied in symmetric collisions of ^{36}Ar+KCl (at 32A, 40A, 52A and 74A MeV) [28], ^{58}Ni+^{58}Ni (at 32A, 40A, 52A, 63A, 74A, 82A and 90A MeV) [28], ^{129}Xe+^{118}Sn (at 25A, 32A, 40A, 45A and 50A MeV) [29], ^{181}Ta+^{197}Au (at 33A, 39A MeV) and ^{238}U+^{238}U (at 24A MeV) [28]. On the other hand entrance channel effects are studied by keeping the total mass equal to 250 units. Naturally, for studying the gentle compression and Coulomb instabilities, they have to go to heavy fragments. The collisions of light systems leads to the vaporization. Recently, a detailed theoretical study of INDRA experimental findings was carried out by Aichelin and coworkers [30].

The Berkley group has concentrated mainly on the asymmetric reactions like ^{197}Au+^{27}Al, ^{51}V and ^{64}Cu at 60A MeV or ^{36}Ar+^{197}Au at 50A and 110A MeV, ^{56}Fe+^{197}Au at 50A and 100A MeV, ^{139}La+^{12}C at 50A, 80A and 100A MeV, and ^{139}La+^{12}C, ^{27}Al, ^{40}Ca, ^{64}Cu, ^{139}La at 35A,40A,45A and 55A MeV etc. They concentrated on different probabilities which include the excitation energy, the angular distribution and the velocity distribution etc. Another symmetric reactions studied were carried out using AMPHORA detector at SARA (France) [31].

The MSU group studied the reactions like ^{36}Ar+^{197}Au, ^{129}Xe+^{197}Au at 50A-110A MeV , ^{129}Xe+^{12}C, ^{27}Al, ^{51}V, ^{64}Cu, ^{89}Y, ^{197}Au at 50A MeV, ^{197}Au+^{197}Au at 100A-400A MeV, ^{40}Ar+^{197}Au at 35A, 50A, 80A and 110A MeV [32,33] etc. To understand the underlying physics, several statistical and dynamical models were also employed.

The FOPI and ALADIN groups at GSI are studying the variety of reactions giving nearly all kinds of possibilities. It ranges from ^{12}C to ^{208}Pb and with incident energy between 100A and 1000A MeV. A lot of physical conclusions are also drawn from these studies. The above mentioned experiments are some of the important experiments performed in recent years.

The ALADIN group reported a target independence if fragment multiplicities are plotted against Z_{bound} ,(=the sum of charges of all fragments with $Z \geq 2$). This is valid at energies above 600A MeV. This is true if projectile is fixed and target is changed. Naturally if projectiles are different then one has to rescale everything with the charge of the projectile. In addition to above facts different experiments gave indications that the impact parameter can be closely related with the emission of charged particles, thus making it possible to extract the impact parameter experimentally.

Theoretically several models have been developed which makes the situation more complicated. The heavy ion collisions involve very complicated non equilibrium physics, therefore, its numerical modeling is not straight forward. Due to lack of free phase-space at low incident energies about 98% of attempted collisions are blocked. The whole dynamics at low energies is governed by the mean field or by the mutual two and three body interactions. In contrary, the availability of large free phase space at relativistic energy (≥2A GeV) makes the Pauli principle's role quite small (roughly 4% collisions are blocked) and hence the dynamics of the reaction is governed by Cascade picture.

The semi classical version of extended time dependent Hartree-Fock theory (ETDHF) i.e Vlasov equation was coupled with nucleon-nucleon collisions and thus a new realization named as Boltzmann-Uehling-Uhlenbeck equation(BUU) is used till date to study the large deviating problems of low, intermediate and relativistic heavy ion collisions. Many more names like Landau-Vlasov (LV) equation [34] or Vlasov-Uehling-Uhlenbeck (VUU) [35] or Boltzmann-Nordheim equation [36] also exist for the same realization. The solution of BUU equation provides the time evolution of one body distribution function in six dimensional phase space. In actual calculation one does not solve the BUU equation directly, instead one solves the classical Hamiltonian equations of motion for the propagation of particles in mean field. The two body collisions (and the

Pauli principle) are treated in a rather phenomenological way by employing the Monte-Carlo technique. Due to one body nature, BUU cannot describe correctly, for example, the multi-fragmentation phenomenon which involves the correlations between nucleons. Recently, some attempts were made to extend the BUU equation by including stochastic two body correlations so that the N-body phenomena like multi-fragmentation can also be studied.

Naturally, one would like to have the methods where correlations and fluctuations among the nucleons can be preserved. The classical molecular dynamics (MD) approach (or the equation of motion), in principle, is capable of treating both the compression and the fragment formation. The molecular dynamics predicts the collective (sidewards) flow in a qualitative agreement with the data. It incorporates the complete classical N-body dynamics which is necessary to describe the formation of the fragments. The quantum features play very important role at low energies. This approach was later extended to incorporate the quantum features by Aichelin and Stocker [37]. This new approach which explicitly incorporates the N-body correlations, a nuclear equation of state and important quantum features (like Pauli-principle, stochastic scattering and particle production) was dubbed as Quantum Molecular Dynamics (QMD) model. The crucial quantum features like antisymmetrization etc. were implemented in approaches like Fermionic Molecular Dynamics (FMD) and Antisymmetric Molecular Dynamics (AMD). The serious numerical problems have restricted the use of FMD and AMD approaches to light nuclei only.

The dynamical models can follow the phase space of nucleons and are capable of studying the various experimental observables. All these dynamic models follow the time evolution of the nucleons only, and therefore one needs a procedure to define the clusters. The nucleons were connected to cluster using space correlation method. This method identifies two nucleons in a same fragment if their centroids are less than some distance [38]. This method is also called as Minimum Spanning Tree (MST) method. Naturally, this definition is valid when the system is dilute and thus it cannot address the question of mechanism behind the multifragmentation which may happen at high energies. Several refinements to this method were proposed later on. This method is one of the most extensively used methods. Recently this method when coupled with QMD model failed to explain the observed fragment distribution obtained by ALADIN group [39].

This failure was more pronounced in peripheral collisions where in contrast to energy transferred in QMD from participant to spectator matter was not enough to break the spectator into pieces. So alternative searches were made.

From the discussion, it is clear that several theoretical tools are available. As our present interest is to understand the formation of fragments, we shall study the dynamics of fragmentation using QMD model. A lot of efforts are being made to compare the QMD + MST calculations with experimental data

1.2 Motive of the work

Motive of our work was to compare our theoretical findings with available experimental data in intermediate energy heavy ion collisions. Experimental data was available for intermediate mass fragments at different energies of ALADIN collaboration. Following the same work we obtained the theoretical data for Au-Au heavy ion collisions under the similar conditions as were for ALADIN experiment and obtained the results which were in good agreement with the experimental data.

1.3 References

[1] H. Stocker and W. Greiner, Phys. Rep. **137**, 277 (1986).

[2] D.H.E. Gross. Rep. Prog. Phys. **53**; 605 (1990).

[3] J.P. Bondorf, A. S. Botvina and I. N. Mishustin, Phys Rep**. 257**; 133 (1995).

[4] W.Stocker, Phys.Lett. B**142**; 319 (1984).

[5] M.L. Gilkes et al., Phys. Rev. Lett. **73**; 1590 (1996).

[6] A. Schuttauf et al. , Nucl. Phys. A**607** (1996) 457.

[7] M. Begemann-Blaich et al., Phys. Rev. C**58** (1998), 1639.

[8] J E Finn *et al*, *Phys. Rev. Lett.* **49**, 1321 (1982)

[9] R W Minich *et al*, *Phys. Lett.* **B118**, 458 (1982)

[10] M E Fisher, *Physica* **3**, 255 (1967)

[11] N T Porile *et al*, *Phys. Rev.* **C39**, 1914 (1989)

[12] M L Gilkes *et al*, *Phys. Rev. Lett.* **73**, 1590 (1994)

[13] J A Hauger *et al*, *Phys. Rev. Lett.* **77**, 235 (1996)

[14] J B Elliott *et al*, *Phys. Lett.* **B381**, 35 (1996)

[15] J A Hauger *et al*, *Phys. Rev.* **C57**, 764 (1998)

[16] J B Elliott *et al*, *Phys. Lett.* **B418**, 34 (1998)

[17] B K Srivastava *et al*, *Phys. Rev.* **C60**, 064606 (1999)

[18] R P Scharenberg *et al*, submitted to *Phys. Rev.* **C**

[19] J Bondorf *et al*, *Phys. Rep.* **257**, 133 (1995)

[20] D H E Gross, *Phys. Rep.* **279**, 119 (1997)

[21] S Das Gupta and A Z Mekjian, *Phys. Rev.* **C57**, 1361 (1998)

[22] S Das Gupta *et al*, *Nucl. Phys.* **A621**, 897 (1997)

[23] J M Carmona, J. Richert, A. Tarancon and P. Wagner, *Nucl. Phys.* **A643**, 115 (1998)

[24] F Gulminelli and Ph Chomaz, *Phys. Rev. Lett.* **82**, 1402 (1999)

[25] S. Koonin, Ph.D. thesis, MIT (1975)

[26] J. P. Bondorf, H. T. Feldmeier, S. Garpman and E. C. Halbert, Phys. Lett. B**65**, 217(1976)

[27] E.Suraud, Ch. Gregoire and B. Tamian, Prog. Part. Nucl. Phys. **23**, 357 (1989).

[28] J. Cugnon, T. Mizutani and J. Vandermeulen, Nucl. Phys. A**352**, 505 (1981)

[29] S. D. Gupta, C. Gale and J. Gallego, Phys. Rev. C**33**, 1634 (1986)

[30] G. Bertesch and J. Cugnon, Phys. Rev. C**24**, 2514 (1981)

[31] J. Cugnon and D. L'Hote, Phys. Lett. B**149**, 35 (1984)

[32] W. Bauer, G. F. Betsch, W. Cassing and U. Mosel, Phys. Rev. C**34**, 2127 (1986)

[33] W. Bauer, Phys. Rev. Lett. 61, 2534 (1988); ibid Nucl. Phys. A**471**, 604 (1987)

[34] R. K. Puri, E. Lehmann, A. Faessler and S. W. Huang, J. Phys. G**21**, 583 (1995)

[35] A. Jahns, C. Spieles, R. Mattielo, H. Stocker, W. Greiner and H. Sorge, Phys. Lett. B**308**, 11 (1993)

[36] A. Jahns, H. Stocker, W. Greiner and H. Sorge, Phys. Rev. Lett. **68**, 2895 (1992)

[37] J. Aichelin and H. Stocker, Phys. Lett. B**176**, 14 (1986)

[38] J. Aichelin, Phys. Reports, **202**, 233 (1991)

[39] M. Begemann-Blaich et al., Phys. Rev. C**48**, 610 (1993)

Chapter 2

Methodology

The study of intermediate energy heavy ion collision needs correct treatment of the real and imaginary parts of nuclear interactions. The real part influences the trajectory of nucleons whereas the imaginary part deals with the nucleon-nucleon collisions. In the following we first present the Vlasov-Uehling-Uhlenbeck (VUU) theory and then discuss the Intra Nuclear Cascade (INC) model, the Quantum Molecular Dynamics (QMD) model.

2.1 Vlasov-Uehling-Uhlenbeck (VUU) theory

The microscopic transport models for the one-body Wigner phase space density distribution obtained different names although they solve the same equation. These models differ in the technical realization, i.e. the computer program, and are known as Vlasov-Uehling-Uhlenbeck (VUU) model (or BUU [1,2], LV [3]). The transport equation has been solved for the one-body Wigner density $f(\boldsymbol{r}; \boldsymbol{p}; t)$ in the limit $\hbar \to 0$:

$$\frac{\partial f}{\partial t} + v.\boldsymbol{\nabla}_r f - \boldsymbol{\nabla}_r U.\boldsymbol{\nabla}_p f = -\frac{4\pi^3(\hbar c)^4}{\hbar(mc^2)^2} * \int \frac{d^3p_1'}{(2\pi\hbar)^3}\frac{d^3p_2'}{(2\pi\hbar)^3} d^3p_2 \frac{d\sigma}{d\Omega} * [ff_2(1-f_1')(1-f_2') - f_1'f_2'(1-f)(1-f_2)] * \delta^3(p + p_1 - p_2' - p_1') \quad (1)$$

The l.h.s. of this equation is the total differential of *f* with respect to the time assuming a momentum independent potential *U*. This potential is calculated selfconsistently and corresponds to the real part of the Bruckner G-matrix. Usually a Skyrme-parametrization

$$U = \alpha\left(\frac{\rho}{\rho_0}\right) + \beta\left(\frac{\rho}{\rho_0}\right)^{\Upsilon} \quad (2)$$

of the real part of the G-matrix is employed, where ρ is the nuclear density which is frequently measured in units of the saturation density ρ_0 of cold nuclear matter. The r.h.s. of eq. (1) contains a Boltzmann collision integral, which is identified with the imaginary part of the G-matrix. This part describes the influence of binary hardcore collisions, where the term with f f_2 describes the loss of particles (in a phase space region) and the term with $f_1' f_2'$ the gain term due to collisions feeding the considered phase space region. It is supplemented with the Nordheim-Uehling-Uhlenbeck modifications in order to obey the Pauli-principle in the final state of the collisions [4]. The δ-functions assure the conservation of the four-momentum.The cross section $\boldsymbol{\sigma}$ is normally adjusted to the free nucleon-nucleon scattering. The differences from cross sections calculated from the imaginary part of the Bruckner G-matrix are minor [5] and influence little the observables of a heavy ion collision. The equation is solved by use of the test particle method. Here the continuous one-body distribution function *f* at *t* = 0 is represented by an ensemble of *n.*(A_p + A_t) pointlike particles. This is often viewed as an ensemble of *n* parallel events with A_p + A_t physical particles each, where A_p and A_t denote the number of nucleons in projectile and target, respectively. The l.h.s. of eq. (1) can be regarded as the transport equation (Vlasov-equation) for the distribution of classical particles whose time evolution is governed by Hamilton's equations of motion.

$$\dot{p_i} = -\frac{\partial \langle H \rangle}{\partial r_i} \quad \text{and} \quad \dot{r_i} = \frac{\partial \langle H \rangle}{\partial p_i} \tag{3}$$

The testparticles move due to their own, selfconsistently generated mean-field. The r.h.s. is taken into account by additional stochastic scattering similar to the collisions in cascade models [6,7].

More explicitly the test particle method corresponds to the replacement of the expectation value of a single particle observable

$$\langle O(t) \rangle = \int f(r,p,t)\, O(r,p) d^3r\, d^3p \tag{4}$$

by a Monte Carlo integration

$$\langle O(t)\rangle = \frac{1}{n(A_T+A_P)}\sum_{i=1}^{n(A_T+A_P)} O(r_i(t),\, p_i(t)) \qquad (5)$$

where the $\boldsymbol{r}_i(t)$ and $\boldsymbol{p}_i(t)$ are points in phase space which are distributed according to $f(\boldsymbol{p}; \boldsymbol{r}; t)$, i.e.,

$$f(\boldsymbol{p}; \boldsymbol{r}; t) = \lim_{n\to\infty} \frac{1}{n(A_T+A_P)}\sum_{i=1}^{n(A_T+A_P)} \delta(r - r_i(t))\,\delta(p - p_i(t)) \qquad (6)$$

The numerical realization can be achieved in various ways. VUU uses a phase space sphere around each particle in order to determine *f* and a coordinate space sphere to determine ρ and thus *U*(ρ). This corresponds to a Lagrangian method. On the contrary, BUU uses a fixed grid corresponding to an Eulerian method in hydrodynamics. In both models collisions are treated in a parallel event method, only. The Landau-Vlasov model determines *f* by the overlap of several Gaussians. The collisions are performed in a crossedevent (or full ensemble) method where all $n(A_p + A_t)$ may collide with each other with a scaled cross section.

For a solution of (1) proper boundary conditions have to be specified. In the case of heavy ion reactions, the test particles are distributed according to the density- and (Fermi-) momentum distribution of ground state nuclei. The later are then boosted onto every other with the proper relative momentum. Initially the test particles are randomly distributed in a coordinate space sphere of the radius $R = 1.12A^{1/3}$ fm (where A is the atomic number of the nucleus) and in a momentum space sphere of the radius of the corresponding Fermi momentum.

One should keep in mind that the forces acting on the test particles are calculated from the entire distribution including test particles from all events, hence the *n* parallel events are not independent and event-by-event correlations cannot be analyzed within this one-body transport models. In the limit $n \longrightarrow \infty$ the distribution of these propagated test particles at the time *t* represents the one-body distribution function at this time. Any one-body observable can be calculated by averaging the values weighted with

the distribution function according to (5). Hence, VUU type models succeeded in the description of one body observables like collective flow, stopping and particle spectra, but, fluctuations and correlations, such as the formation of fragments or the description of two-particle correlations in relativistic heavy ion collisions, are beyond the scope of a transport model based on a one-body distribution function [8,9]. Any fluctuation of the observables seen in the Monte Carlo simulation of the One-body distribution function is due to numerical noise and disappears in the limit of a infinite number of test particles.

2.2 The Intra Nuclear Cascade (INC) Model

At intermediate energies, the mean field and two body nucleon-nucleon collisions play an equally important role in the evolution if the system. The INC model is capable of describing the heavy ion collisions [10]. In this model the mean field is totally neglected and the nucleon-nucleon (NN) collisions are taken without Pauli-blocking [11,12,13,14]. Note that this was the first microscopic dynamical model used to understand the experimental data of heavy ion collisions [10]. The Cascade model simulates the heavy ion collisions as superposition of independent two body NN collisions. Naturally, in the absence of mean field, the nucleons move on straight line trajectories until they collide.

In INC model, each nucleus is considered as collection of point particles distributed within a sphere without any Fermi momentum. When two nuclei approach each other, the position of each nucleon is assigned by Monte-Carlo sampling. The time evolution is followed by dividing the whole reaction time into small intervals Δt. Two nucleons are supposed to collide if they pass the point of closest approach within a given time interval. The distance of closest approach d_{max} is $\sqrt{\sigma_{nn}^{t}(\sqrt{s})/\Pi}$ with $\sigma_{nn}^{t}(\sqrt{s})$ as the total nucleon-nucleon cross section in their centre-of-mass system and $\sqrt{s}$ is the centre-of-mass energy. The colliding particles can also scatter elastically or inelastically. The main processes include:

$$\text{Elastic} \qquad \begin{aligned} N + N &\longrightarrow N + N \quad (a) \\ N + \Delta &\longrightarrow N + \Delta \quad (b) \\ \Delta + \Delta &\longrightarrow \Delta + \Delta \quad (c) \end{aligned} \tag{7}$$

inelastic $N + N \longrightarrow N + \Delta$ (d)

$N + \Delta \longrightarrow N + N$ (e) (8)

The cross sections for channel (a) and (d) are taken from experiments. The cross section for channel (e) is obtained by detailed balance method. The cross section for channel (b) and (c) are taken to be same as (a).

At the end of the simulations, all Δ's decay isotropically into nucleons and pions by conserving the charge, isospin quantum number. In other words, the number of Δ's at the end of reaction gives the number of pions.

One can also calculate the entropy generated in a nuclear system after the collision. The entropy for non interacting Fermionic system is given by

$$S = - \int d\gamma [f \ln f + (1 - f) \ln(1 - f)], \quad (9)$$

Here f is the occupation probability in the phase-space which is given by $f = \frac{N}{R}$, with R being the total number of events and N are the number of the particles in a given cell. The $d\gamma$ is the phase space volume element given by $\int d\gamma = \int \frac{d^3r d^3p}{(2\pi\hbar)^3}$. To calculate f, the whole phase space is divided into cells i. The distribution function f is then estimated by relation

$$f = \frac{n_i}{R \int d\gamma} \quad (10)$$

The INC gave excellent opportunity to extract the information about several experimental observables [10]. As the INC does not contain the mean field of nucleons, it is more suitable for high energy experiments.

2.3 The Quantum Molecular Dynamics (QMD) approach

An approach which goes beyond a one-body description as explained above, is the Quantum Molecular Dynamics (QMD) model. The QMD model is a *n*-body theory which simulates heavy ion reactions at intermediate energies on an event by event basis. Taking

into account all fluctuations and correlations has basically two advantages: i) many-body processes, in particular the formation of complex fragments are explicitly treated and ii) the model allows for an event-by-event analysis of heavy ion reactions similar to the methods which are used for the analysis of exclusive high acceptance data.

2.3.1 Formal derivation of the transport equation:

In QMD each nucleon is represented by a coherent state of the form (we set ħ,*c* = 1) which are characterized by six time-dependent parameters, $\boldsymbol{r}_i$ and $\boldsymbol{p}_i$, respectively.

$$\Phi_i(x_i;t) = \left(\frac{2}{L\pi}\right)^{3/4} e^{-(x_i - r_i(t))^2/L}\, e^{i x_i p_i(t)} \tag{11}$$

The parameter *L*, which is related to the extension of the wave packet in phase space, is fixed. The total *n*-body wave function is assumed to be the direct product of coherent states

$$\Phi = \prod_i \phi_i(x_i, r_i, p_i, t) \tag{12}$$

Note that we do not use a Slater determinant (with $(A_p+A_t)!$ summation terms) and thus neglect antisymmetrization. First successful attempts to simulate heavy ion reactions with antisymmetrized states have been performed for small systems [15,16]. A consistent derivation of the QMD equations of motion for the wave function under the influence of both, the real and the imaginary part of the G-matrix, however, has not yet been achieved. Therefore we add the imaginary part as a cross section and treat them as in the cascade approach. How to incorporate cross sections into a antisymmetrized molecular dynamics is not yet known. This limits its applicability to very low beam energies.

The initial values of the parameters are chosen in a way that the ensemble of $A_T + A_P$ nucleons gives a proper density distribution as well as a proper momentum distribution of the projectile and target nuclei.

The equations of motion of the many-body system is calculated by means of a generalized variational principle:

we start out from the action

$$S = \int_{t_1}^{t_2} \mathcal{L}[\Phi, \Phi^*] dt \tag{13}$$

with the Lagrange functional

$$\mathcal{L} = \left\langle \Phi \left| i\hbar \frac{d}{dt} - H \right| \Phi \right\rangle \tag{14}$$

where the total time derivative includes the derivation with respect to the parameters. The Hamiltonian *H* contains a kinetic term and mutual interactions V_{ij} , which can be interpreted as the real part of the Bruckner G-matrix supplemented by the Coulomb interaction.

$$\begin{aligned} \langle H \rangle &= \langle T \rangle + \langle V \rangle \\ &= \sum_i \frac{p_i^2}{2m_i} + \sum_i \sum_{j>i} \int f_i(\boldsymbol{r}, \boldsymbol{p}, t)\, V^{ij} \\ &\qquad \times f_i(\boldsymbol{r}', \boldsymbol{p}', t)\, d\boldsymbol{r}\, d\boldsymbol{r}' d\boldsymbol{p}\, d\boldsymbol{p}'. \end{aligned} \tag{15}$$

Where the Wigner distribution f_i of the nucleon i can be easily derived from the test wave functions (antisymmetrization is neglected).

$$f_i(\boldsymbol{r}, \boldsymbol{p}, t) = \frac{1}{\pi^3 \hbar^3} \mathrm{e}^{-(\boldsymbol{r}-\boldsymbol{r}_i(t))^2 \frac{2}{L}} \mathrm{e}^{-(\boldsymbol{p}-\boldsymbol{p}_i(t))^2 \frac{L}{2\hbar^2}} \tag{16}$$

The baryon-potential consists of the real part of the *G*-Matrix which is supplemented by the Coulomb interaction between the charged particles. The former can be further subdivided in a part containing the contact Skyrme type interaction only,

contribution due to a finite range Yukawa-potential, and a momentum dependent part $V^{ij} = G^{ij} + V^{ij}_{Yuk} + V^{ij}_{Coul} + V^{ij}_{mdi}$ consists of

$$\begin{aligned} V^{ij} &= G^{ij} + V^{ij}_{\mathrm{Coul}} \\ &= V^{ij}_{\mathrm{Skyrme}} + V^{ij}_{\mathrm{Yuk}} + V^{ij}_{\mathrm{mdi}} + V^{ij}_{\mathrm{Coul}} \\ &= t_1\delta(\boldsymbol{x}_i - \boldsymbol{x}_j) + t_2\delta(\boldsymbol{x}_i - \boldsymbol{x}_j)\rho^{\gamma-1}(\boldsymbol{x}_i) \\ &\quad + t_3\frac{\exp\{-|\boldsymbol{x}_i - \boldsymbol{x}_j|/\mu\}}{|\boldsymbol{x}_i - \boldsymbol{x}_j|/\mu} + \\ &+ t_4\ln^2(1 + t_5(\boldsymbol{p}_i - \boldsymbol{p}_j)^2)\delta(\boldsymbol{x}_i - \boldsymbol{x}_j) + \frac{Z_i Z_j e^2}{|\boldsymbol{x}_i - \boldsymbol{x}_j|} \end{aligned} \tag{17}$$

Z_i; Z_j are the charges of the baryons i and j. The real part of the Bruckner G-matrix is density dependent, which is reflected in the expression for G^{ij} . The expectation value of *G* for the nucleon *i* is a function of the interaction density ρ^i_{int}. It is indeed this quantity which relates the number density to the energy content of nuclear matter.

$$\rho^i_{\mathrm{int}}(\boldsymbol{r}_i) = \frac{1}{(\pi L)^{3/2}}\sum_{j\neq i}\mathrm{e}^{-(\boldsymbol{r}_i - \boldsymbol{r}_j)^2/L} \tag{18}$$

The time evolution of the parameters is obtained by the requirement that the action is stationary under the allowed variation of the wave function. This yields an Euler-Lagrange equation for each parameter.

If the true solution of the Schrodinger equation is contained in the restricted set of wave functions $\phi_i(\mathbf{x}_i; t)$ (with parameters $r_i;p_i$) this variation of the action gives the exact solution of the Schrodinger equation. If the parameter space is too restricted, the wave function in the restricted parameter space which comes closest to the solution of the Schrodinger equation. The set of wave functions which can be covered with spatial parametrizations is not necessarily a subspace of Hilbert-space, thus the superposition principle does not hold.

2.3.2 Inclusion of collisions

As stated before the imaginary part of the G-matrix acts like a collision term. In the QMD simulation we restrict ourselves to binary collisions (two-body level). The collisions are performed in a point-particle sense in a similar way as in VUU or cascade: Two particles collide if their minimum distance *d*, i.e. the minimum relative distance of the centroids of the Gaussians during their motion, their CM frame fulfills the requirement:

$$d \leq d_0 = \sqrt{\frac{\sigma_{\mathrm{tot}}}{\pi}}, \qquad \sigma_{\mathrm{tot}} = \sigma(\sqrt{s},\ \mathrm{type}). \tag{20}$$

where the cross section is assumed to be the free cross section of the regarded collision type (*N* - *N*, *N* - Δ, . . .).

Beside the parameters describing the *N*-*N* potential, the cross sections constitute another major part of the model. In principle, both sections of parameters are connected and can be deduced from Bruckner theory. QMD calculations using consistently derived cross sections and potentials from the local phase space distributions have been discussed e.g. in [19]. Such simulations are time consuming since the cross-sections and potentials do explicitly depend on the local phase space population.

Within the framework of using free cross section one may parameterize the cross section of the processes to fit the experimental data if available. For unknown cross sections isospin symmetry and time reversibility is assumed.

Alternatively, cross-sections may be obtained from theoretical considerations. For one particular QMD-version the one boson exchange model has been employed for this purpose. This has the advantage to have a first handle for the description of cross sections in the nuclear medium.

2.3.3 Pauli blocking due to Fermi statistics

The cross section is reduced to an effective cross section by the Pauli-blocking. For each collision the phase space densities in the final states are checked in order to

assure that the final distribution in phase space is in agreement with the Pauli principle ($f \leq 1$). Phase space in QMD is not discretized into elementary cells as in one-body models like VUU, in order to obtain smooth distribution functions the following procedure is applied: The phase space density f_i' at the final states 1' and 2' is measured and interpreted as a blocking probability. Thus, the collision is only allowed with a probability of $(1- f_1')(1- f_2')$. If the collision is not allowed the particles remain at their original momenta.

The Pauli blockers of VUU and QMD show effciencies of about 94-96 %, i.e. a single ground state nucleus with Fermi momentum would show a blocking rate of this amount. In order to reduce the noise of spurious collisions in ground state nuclei additional conditions allow a nucleon only to collide with a nucleon of the other nucleus or with a nucleon that has already undergone a collision. Nevertheless the problem of Pauli blocking causes a limitation of the calculated system to have not less incident energy than about the Fermi energy.

2.4 Minimum Spanning Tree (MST) method

In MST [18-24], two nucleons share the same fragments if their centroids are closer than a distance d_{min},

$$|r_i - r_j| \leq d_{min}$$

Where r_i and r_j are the spatial positions of both nucleons. The minimum distance d_{min} has been used as a free parameter which varies between 2-4 fm. Its influence on multifragmentation (at 200-300 fm/c) is reported to be small [25]. This approach (being a spatial distance approach) cannot detect different fragments which are almost overlapping and therefore, will give a single big fragment during the early stage of the reaction where density is quite high and the interactions among the nucleons are still active. In other words, the simple coordinate space approach cannot address the question of time scale of the fragments. To study the time of

fragment formation, one needs to derive a method which should be able to detect the overlapping fragments.

References

[1] G.F. Bertsch, H. Kruse and S. Das Gupta. Phys. Rev. C**29**, R673 (1984)

[2] J. Aichelin and G. Bertsch. Phys. Rev. C**31**, 1730 (1985)

[3] C. Gregoire, B. Remaud, F. Sebille, L. Vinet, and Y. Raffray, Nucl. Phys. A**465**, 317 (1987)

[4] E. A. Uehling and G. E. Uhlenbeck. Phys. Rev. **43**, 55 (1933) and Phys. Rev. **44**, 917 (1934)

[5] A. Bohnet et al. Phys. Rev. C**44**, 2111 (1991)

[6] Y. Yariv and Z. Frankel. Phys. Rev. C**20**, 2227 (1979)

[7] J. Cugnon. Phys. Rev. C**22**, 1885 (1980)

[8] P.B. Gossiaux, D. Keane, S. Wang, and J. Aichelin, Phys.Rev. C**51**, 3357 (1995)

[9] P.B. Gossiaux, and J. Aichelin, Phys. Rev. C -submitted

[10] J. Cugnon, T. Mizutani and J. Vandermeulen, Nucl. Phys. A**352**, 505 (1981).

[11] S. D. Gupta, C. Gale and J. Gallego, Phys. Rev. C**33**, 1634 (1986).

[12] G. Bertsch and J. Cugnon, Phys. Rev. C**24**, 2514 (1981).

[13] J. Cugnon and C. Volant, Z. Phys. A**334**, 435 (1989).

[14] Y. Yariv and Z. Frankel, Phys. Rev. C**20**, 2227 (1979).

[15]. H. Feldmeier. Nucl. Phys. A**515**, 147 (1990).

[16]. A. Ono, H. Horiuchi, T. Maruyama and A. Ohnishi. Phys. Rev. Lett. **68**, 2898 (1992)

[17]. S.M. Kiselew and Y.E. Pokrovskil. Sov. Journ. Nucl. Phys. **38**, 46 (1983)

[18]. J.J. Molitoris, J.B. Hoffer, H. Kruse and H. Stocker. Phys. Rev. Lett. **53**, 899 (1984)

[19]. J. Jaenicke, J. Aichelin, N. Ohtsuka, R. Linden, A. Faessler, Nucl. Phys. A**536**, 201 (1992)

[20]. T. Kodama et al, Phys. Rev. C**29** (1984) 2146

[21]. Ch. Hartnack. PhD thesis, GSI-Report 93-5 (1993)

Chapter 3

Multifragmentation in Au-Au collisions

In the preceding chapters, a detailed heavy ion picture was presented. Breaking of nuclear matter into pieces is known as multifragmentation.

Multifragmentation depends crucially on several externally controlled parameters as well as on internal model ingredients. It is also dependent on the incident energy, impact parameter, equation of state, nn cross sections. The density profiles of colliding nuclei, momentum dependence of the equation of state and Gaussian width of nucleons have also been reported to have a sizeable effect on formation of fragments.

3.1 Results and discussion

For the present study, we have simulated Au-Au collisions by using Quantum Molecular Dynamics (QMD) model at incident energies ranging from 400 to 1000 MeV/nucleon. The collision geometry used is from central to peripheral one. The phase space obtained from QMD model is analyzed by using minimum spanning tree (MST) algorithm. The results obtained are discussed in the following section.

3.1.1 Time evolution of density and rate of nucleon-nucleon collisions

The final form of the nuclear matter is closely related to the density of the collision. We define the average density as

$$\langle \rho(r_i) \rangle = \langle \sum_j \frac{1}{(2\pi L)^{3/2}} e^{-(r_i - r_j)^2/2L} \rangle$$

This definition shows the number of collisions in the vicinity of each nucleon. Figure 3.1 shows the evolution of scaled density $\langle \rho/\rho_0 \rangle$ with time and rate of collision with time [1]. All the three curves contain rates of collisions at different energies and we consider the case of central collisions only. It is observed that in both figures peaks are observed at almost same time. We notice that density is closely related with rate if collisions. Density is quite different at different energies. It may also be noted that density is maximum at 400 MeV and as we move on increasing the bombarding energy it goes on decreasing. Also rate of collisions vary upto 80-90 fm/c thereafter it gets constant and as a result density varies upto 70-80 fm/c before getting a constant. So naturally the density depends strongly on number of collisions. At high energy the influence of Pauli blocking is less so more number of collisions are allowed, which results in less density.

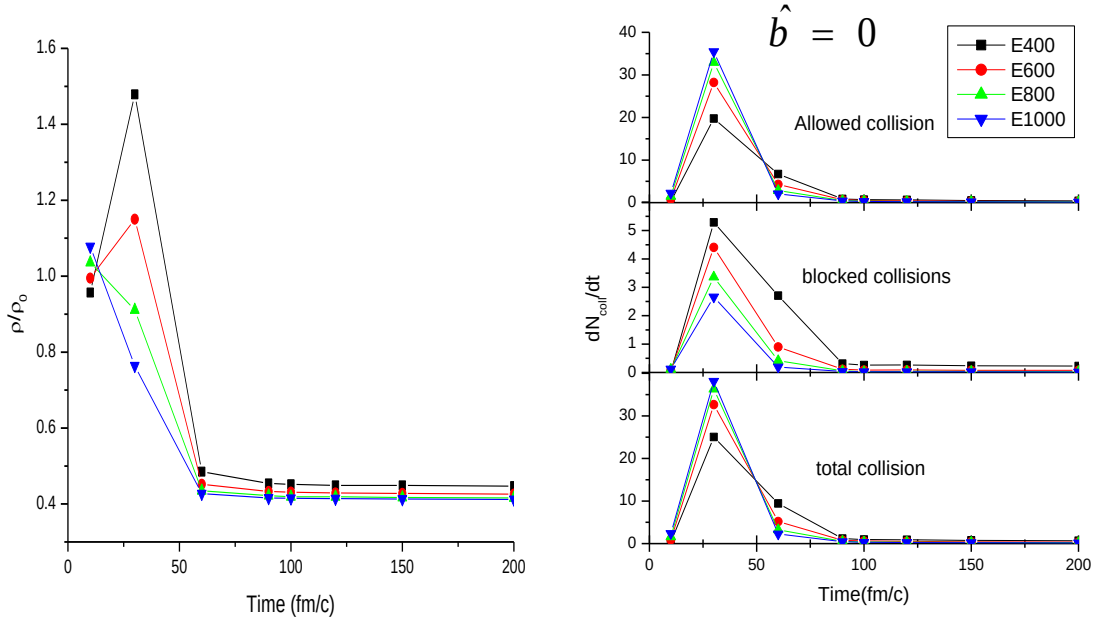

Figure 3.1: Time evolution of scaled density and rate of nucleon-nucleon collisions. Here different lines show the results obtained at different energies.

3.1.2 Time evolution of fragments at central collisions

The formation of the fragments and their multiplicities are discussed in Fig.3.2. The displayed results are at 400, 600, 800 and1000 MeV/nucl. We here display the emitted free nucleons, the light mass fragments (LMF's) (2<*A*<4), the medium mass fragments (MMF's)

(5<*A*<9), and the intermediate mass fragments (IMF's) (5<*A*<66) at central impact parameter. The multiplicity of free nucleons saturate at about 200 fm/c but shows decays in cases of LMF's, MMF's, and IMF's after approaching a sharp peak in each case. This is due to unstability of MMF's and IMF's, which becomes stable by decaying into small fragments.

With increase in incident energy, the multiplicity goes on decreasing except free nucleons. This is due to formation of more compressed zone with the increase in incident energy. This

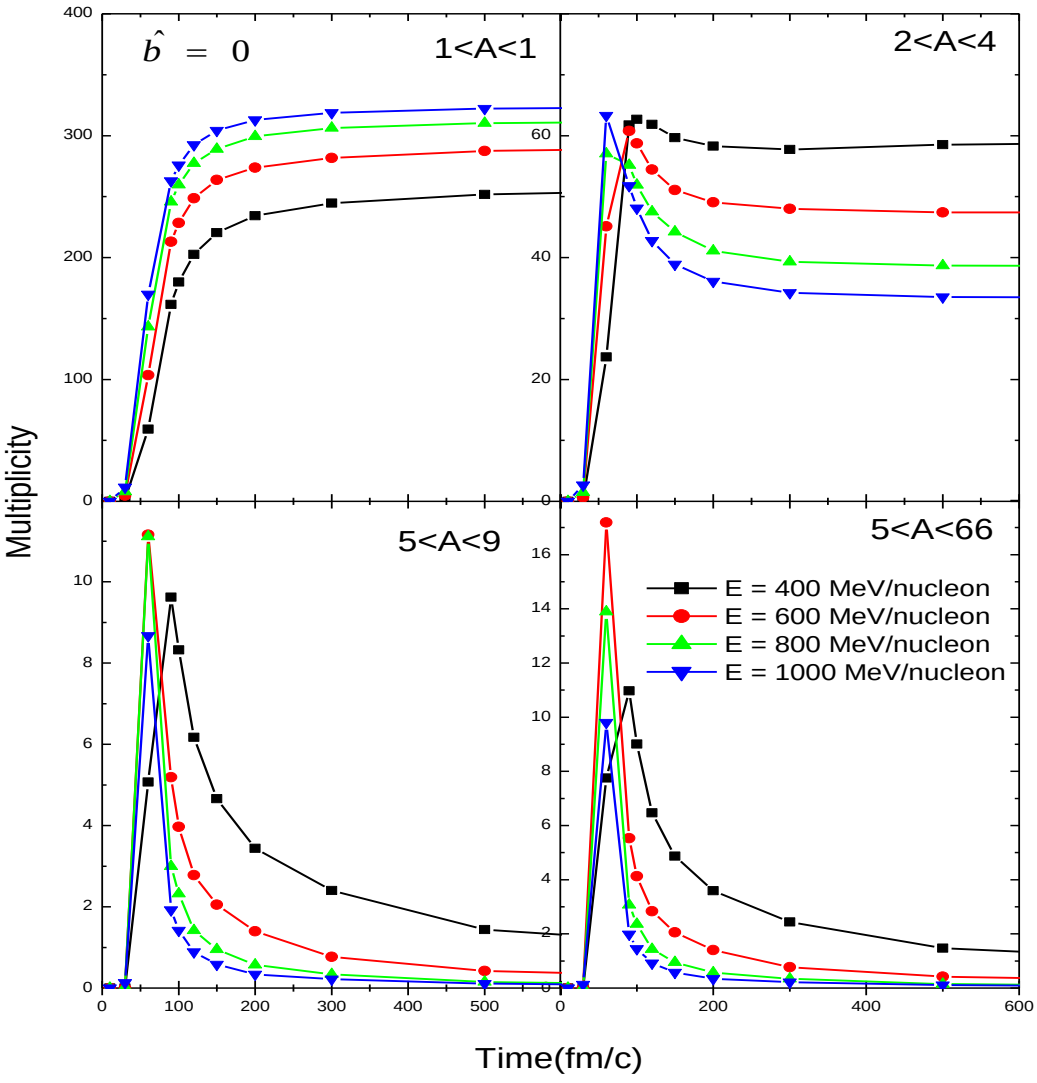

Figure 3.2: The evolution of the central collisions of Au-Au. The time evolution of free nucleons (1 ≤ A ≤ 1), LMF's (2 ≤ A ≤ 4), MLF's (5 ≤ A ≤ 9), IMF's (5 ≤ A ≤ 66) is shown.

compressed zone occurs at central and near central collisions and at high energies and it leads to formation of free particles reducing the formation of fragments..

We observe a delayed emission of all type of fragments using MST method which is due to the fact that until about 40 fm/c, there is just a single fragment in the MST method. The normal MST method depends on the spatial distance. Due to frequent nucleon-nucleon collisions in central collision gemetry, an appreciable part of the nuclear matter is in the form of emitted nucleons and most of initial correlations among nucleons are destroyed which leads to the creation of unstable/unbound fragments. These fragments decay after a while and therefore, one has to follow the reaction dynamics for quite long time to obtain the stable and properly bound fragments. A lot of efforts have been made to avoid the creation of unbound/unstable/weakly bound fragments [2,3,4].

3.1.3 Multiplicity as a function of energy

The effect of different energies on fragmentation pattern is presented in Fig.3.3. The collision of ${}^{197}_{79}Au + {}^{197}_{79}Au$ at different energies ranging from 400 to 1000 MeV is simulated at different impact parameters. Here, we display (1 ≤ A ≤ 1) the free nucleons, (2 ≤ A ≤ 4) the light mass fragments and (5 ≤ A ≤ 66) the intermediate mass fragments (IMF's) as a function of energy.

With the increase in impact parameter the production of free nucleon drastically changes. As the overlap of colliding nuclei decreases, less number of collisions take place and hence free nucleons decrease. Also with increase in energy Pauli blocking effect decreases. The correlations among the nucleons are destroyed at high energies and hence more number of free nucleons are produced.

This effect is largely demonstrated by the lighter fragments. With the increase of energy, more number of clusters manage to qualify as light fragments. As the impact parameter increases, the production of LMF’s falls linearly.

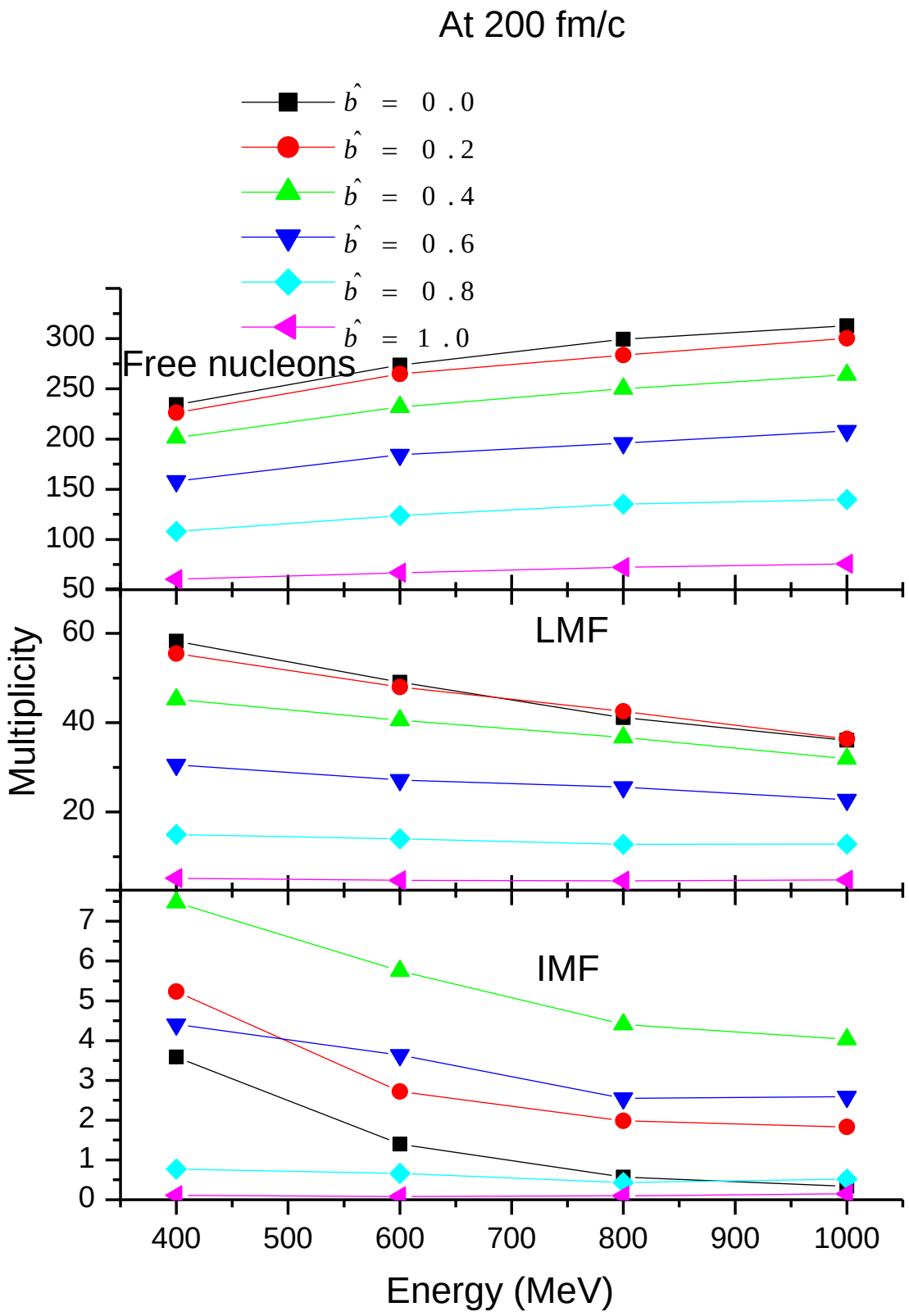

Figure 3.3: Different fragment multiplicities as a function of energy with different impact parameters.

It is seen that multiplicity of intermediate and light mass fragments decrease with the increase in energy but in contrary it goes on increasing with energy for free nucleons. The emission of free nucleons will show disassembly (vaporization) of the matter [5-9].

The production of LMF's is highest at low energy which decreases with the increase in energy. Due to very small overlap at large impact parameter, the system does not receive enough energy and hence cools down after emitting few nucleons/LMF's. The production of IMF's is maximum at low energy and largest impact parameter. The IMF's are preferably produced from the spectator part of the colliding nuclei.

3.1.4 Impact parameter dependence of IMF Multiplicity and Z_{bound}.

Here multiplicity of fragments and charge Z_{bound} as a function of impact parameter has been displayed. It is observed that multiplicity of fragments shows sharp peaks at semi central impact parameters. This is because of the reason that at semi central collisions spectator part of nuclei do not undergo collisions. Thus, for central and peripheral collisions very few IMF's are observed. At central collisions the NN collisions occurring at these energies do not allow any IMF's production whereas at peripheral collisions, not enough energy is transferred from participant to spectator matter, therefore very few IMF's are obtained. We have also carried out a comparison of these theoretical predictions with experimental data reported by ALADIN experiment [10] at energy 400 MeV. It is observed that multiplicity of IMF's shows good agreement with experimental data at low impact parameter while it fails at higher impact parameter. This failure is due method of analysis MST which we had used in our analysis. This is due to the reason that the MST method gives one big cluster at the time of high density. To overcome this failure Puri et al., [11] has performed the analysis with different methods and were successful to explain the experimental data.

Z_{bound} is a parameter in which all the atomic number greater than or equal to 2 are taken into consideration. It is observed that Z_{bnd} goes on increasing with increase in impact parameter. As impact parameter goes on increasing participant matter goes on decreasing while spectator matter goes on increasing, resulting in the formation of fragments having Z>1 and hence increase in Z_{bnd} is obtained. On the other hand, it goes on decreasing with increase in incident energy. This is due to the fact that with increase in incident energy compressed zone becomes hotter resulting in breakup of big fragments into smaller ones resulting in decrease of Z_{bnd} with incident energy. Our results are quantitative in nature with experimental data of ALADIN collaboration. This discrepancy is again due to the method of analysis. Our results clearly indicate that there is a rise and fall in fragment production for central and semi-central collisions with an increase in bombarding energy and also the IMF's multiplicity is maximum at semi central collision and it gradually decreases with increase in impact parameter at all ranges of energies.

3.1.5 Mass and charge distribution

The figure 3.5 displays the mass and charge distribution in different bins. One can see that at low impact parameter and energy the lighter mass fragments are produced but as we increase impact parameter, the spatial overlap decrease and hence production of heavy fragments increases. A bump at large impact parameter is due to heavy fragments produced

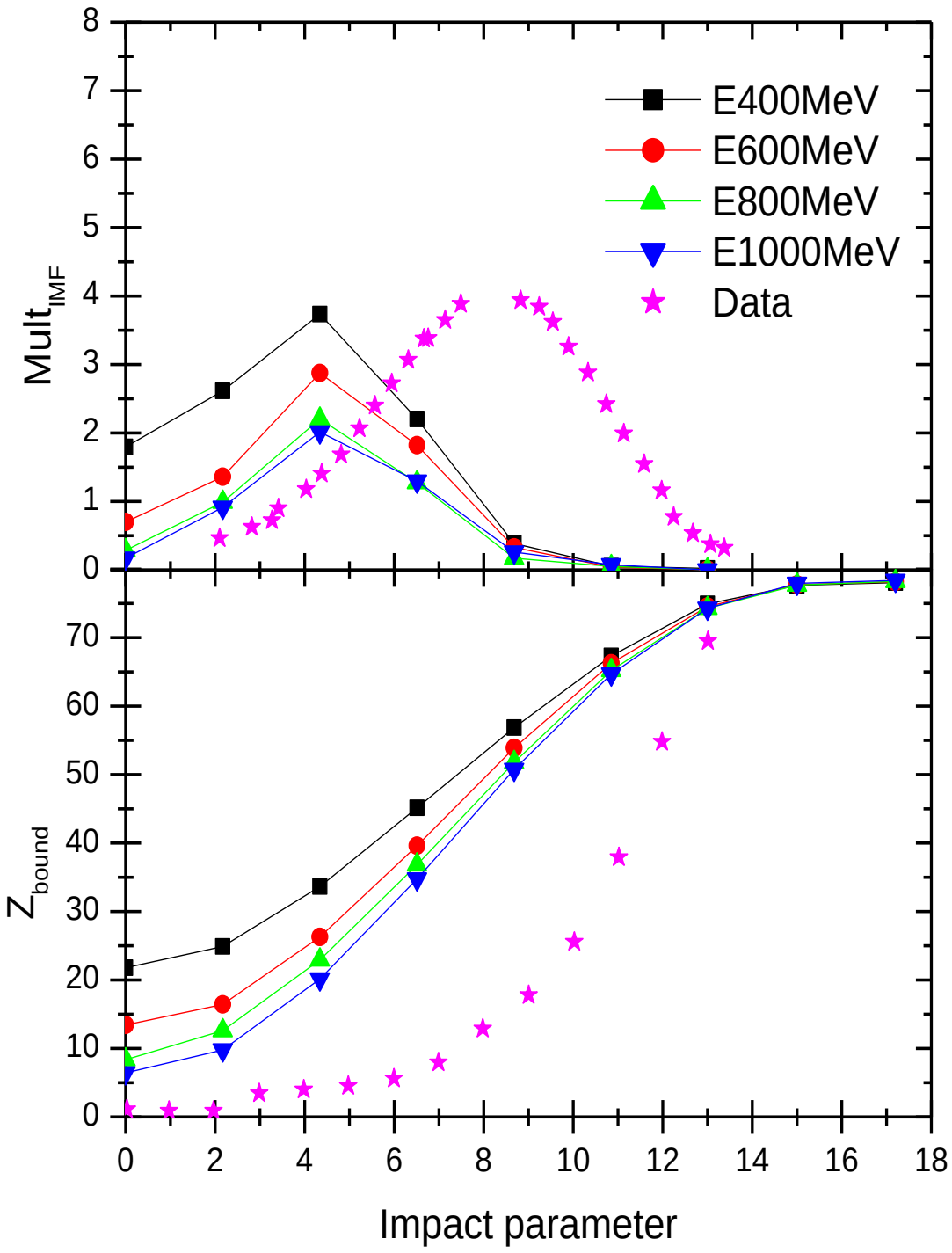

Figure 3.4: Variation of fragment multiplicity and Z_{bnd} with impact parameter at different energies

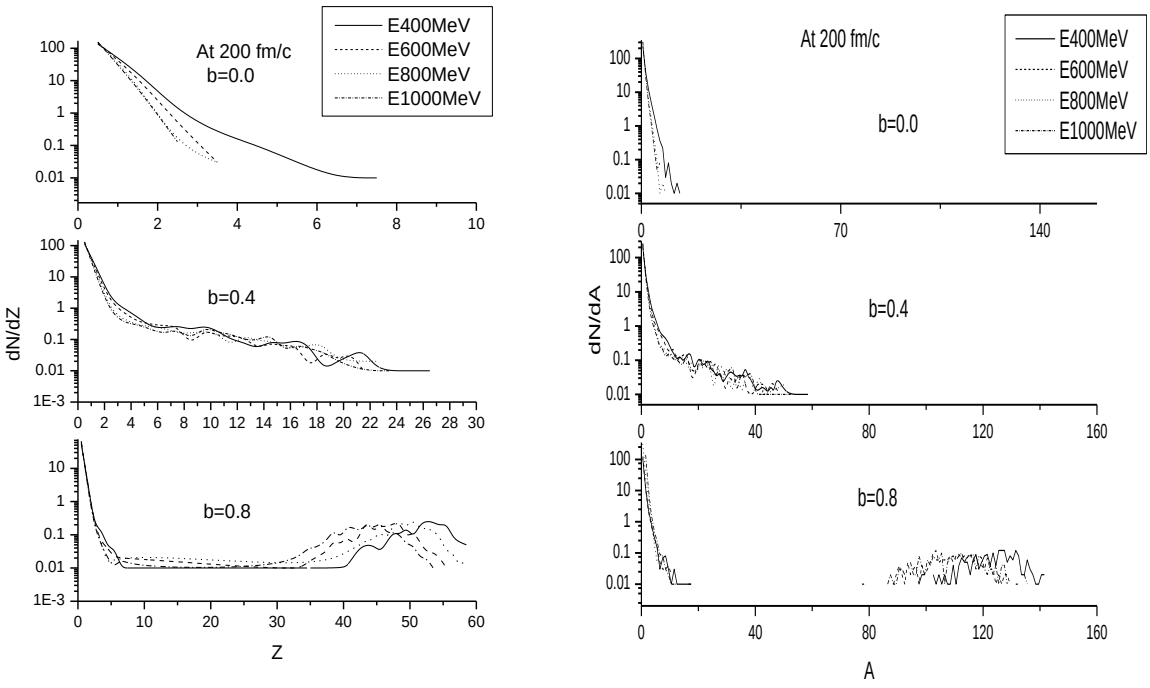

Figure 3.5: Mass and charge distribution of Au-Au collision. The results at different bombarding energies are shown by different lines.

References:

[1] Rajeev K. Puri and Suneel Kumar, Phys. Rev. C 57 (1998) 2744-2747.

[2] S. Kumar and R. K. Puri, Phys. Rev. C 58, 320 (1998); Symposium on Nuclear Phys. 40 B, p.152 (1997).

[3] S. R. Souza, L. de Paula, S. Leray, J. Nemeth, C. Ngo, and H. Ngo, Nucl. Phys. A 571, 159 (1994).

[4] A. Strachan and C. O. Dorso, Phys. Rev. C 56, 995 (1997).

[5] G. F. Peaslee et al., Phys. Rev. C 49, R2271 (1994).

[6] C. Williams et al., Phys. Rev. C 55, R 2132 (1997).

[7] T. Li et al.,Phys. Rev. Lett. 70, 1924 (1992).

[8] N. T. B. Stone et al., Phys. Rev. Lett. 78, 2084 (1997).

[9] B. Jakobsson et al., Nucl. Phys. A 509, 195 (1990).

[10] W. Reisdorf, Prog. Theor. Phys. Suppl.140,111 (2000).

[11] Y. K. Vermani and R. K. Puri, Eur. Phys. Lett. 85, 62001 (2009).

Chapter 4

Summary and outlook

This thesis deals with a theoretical study of multifragmentation. In this thesis, we have presented a theoretical study of multifragmentation in intermediate energy heavy ion collisions. After an introduction to the field of heavy ion physics and multifragmentation, we discussed in **chapter 1**, various experimental and theoretical attempts made to investigate multi-fragmentation.

The details of various theoretical models were discussed in **Chapter 2**. We have discussed, in particular, the *Quantum Molecular Dynamics (QMD)* model used for the present study.

In **chapter 3**, a systematic study of the formation of light and heavy mass fragments was carried out in Au – Au collisions at incident energies between 400 MeV/nucleon – 1000 MeV/nucleon and impact parameter from b=0 to b_{max}. Our aim was to study the dependence of formation of fragments on incident energy and impact parameter. Our results clearly indicate that (i) at central collisions scaled density and collision rate show similar kind of behavior for small spans of time upto a range of 200 fm/c. Also, the density depends strongly on masses of collision rate and (ii) The formation of compressed zone causes the decrease in the production of all types of fragments except free nucleons. We observe rise and fall in the production of intermediate mass fragments with increase in impact parameter. MST can be used to explain the result at low impact parameter, but fails at higher impact parameters.